High Precision Indoor Positioning Method Based on UWB

Janyong Yan, Donghai Lin, Kai Tang, Guangsong Yang(✉), and Qiubo Ye

Jimei University, Xiamen 361021, Fujian, China
gsyang@jmu.edu.cn

Abstract. In order to meet the increasing requirement of indoor positioning, a high precision positioning method based on Ultra Wide Band (UWB) is designed and implemented. Firstly, the ranging method and its improvement are discussed. Secondly, by combining a median filter and Kalman filter algorithm, the collected data are processed by a smooth method to obtain stable ranging data. Finally, an indoor real-time positioning system is realized by using a weighted least square positioning algorithm. Experiment results show that when the refresh frequency is 10 Hz, the ranging accuracy between the base station and the tag can reach 5 cm.

Keywords: Ultra Wide Band · Kalman filtering · Indoor positioning

1 Introduction

A Real Time Location System (RTLS) [1] describes a class of systems that provide information in real-time about the location of objects, animals, people, or just about anything you can imagine. There are many applications of RTLS, for example, tracking and locating assets and patients in healthcare [2]; tracking and locating pallets, packages and items in warehousing and logistics [3]; tracking and monitoring farm animals; and tracking of inventory, work in progress and finished goods in manufacturing environments.

With the development of computer technology and the need of people's quality of life, the demand for positioning accuracy is increasing. Although GPS satellite positioning technology has high accuracy, it is limited by the characteristics of high cost, high power consumption and poor expansibility, neither can it provide effective positioning in indoor and other special areas. Therefore, we need to adopt some mechanisms to achieve precise indoor positioning.

Ultra Wide Band (UWB) [4] is a kind of radio technology based on IEEE 802.15.4a and 802.15.4z standards [5], and the physical properties of the UWB RF signal were specifically defined to achieve real-time, ultra-accurate, ultra-reliable location and communication. The use of complex modulation and demodulation is conducive to reducing costs. UWB uses pulses with nanosecond, which can measure the arrival time of radio waves with high precision and locate the distance with high precision. Because

J. Zheng et al. (Eds.): ADHOCNETS 2019, LNICST 306, pp. 201–207, 2019.
https://doi.org/10.1007/978-3-030-37262-0_16

of the low radiation power density of UWB, it has little effect on a human body. UWB can be widely used in indoor ranging, BAN (Body Area Network) and others fields.

The rest of the paper is organized as follows. In Sect. 2, we describe a ranging method and its improvement. In Sect. 3, we present a smoothing method to smooth the experiment data. Numerical results are given in Sect. 4. Finally, Sect. 5 concludes the paper.

2 Ranging Method and Improvement

There are a number of different methods for implementing RTLS [6], and they usually devolve into two basic types. One is the scheme based on signal strength, which is commonly referred to as RSSI (Received Signal Strength Indication). Another is the time-based method, which is based on the measurement of time it takes for the radio signal to travel between transmitter and receiver. UWB can enable the very accurate measurement of the radio signal propagation time, leading to centimeter accuracy distance/location measurement.

2.1 Two-Way Ranging

Two-way ranging is depicted in Fig. 1. Device A transmits a radio message to Device B and its transmission time (transmit timestamp) t1 is recorded. Device B receives the message and transmits a response (a radio message) back to Device A after a particular delay T_{reply}. Device A then receives this response and records a receive timestamp t2.

Now using the timestamps t1 and t2, Device A can calculate the round trip time T_{round} and know the reply time in the tag, T_{reply}, so $\hat{T}_{\text{prop}}$ can be determined by

$$\hat{T}_{\text{prop}} = \frac{1}{2}(T_{\text{round}} - T_{\text{reply}}) \tag{1}$$

T_{reply} and T_{round} are independently measured using the crystal oscillator of Device A and Device B. Thus, there are offset errors e_A of Device A and e_B of Device B, respectively. The dominant error in the ranging accuracy of this scheme is given by

$$\text{error} = \hat{T}_{\text{prop}} - T_{\text{prop}} \approx \frac{1}{2}(e_B - e_A) * T_{\text{reply}} \tag{2}$$

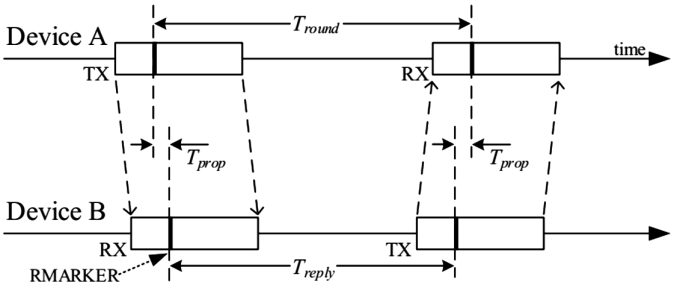

Fig. 1. Two-way ranging

2.2 Symmetric Double-Sided Two-Way Ranging

In the case of two-way ranging, there are a number of error sources due to clock drift and frequency drift. The error in ranging accuracy in the simple two-way ranging scheme is large even with small frequency offsets. An alternative scheme [7] to minimize the error by introducing another message in the ranging transaction is shown in Fig. 2. It reduces the error due to the clock and frequency drift.

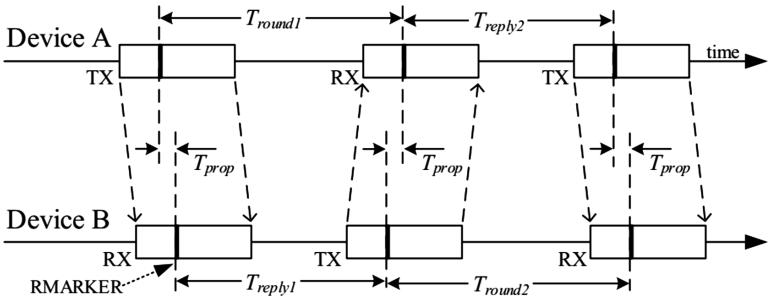

Fig. 2. Symmetric double-sided two-way ranging

In Fig. 2, Device A starts the first round-trip ranging and device B starts the second round-trip ranging. The receiving and transmitting timestamps are recorded and transmitted to device A in the form of data packets for aggregate calculation. Propagation delay can be calculated as

$$\mathrm{T}_{round1} = T_{reply1} + 2 * \hat{T}_{\mathrm{prop}} \tag{3}$$

$$\mathrm{T}_{round2} = T_{reply2} + 2 * \hat{T}_{\mathrm{prop}} \tag{4}$$

Multiplying Eqs. (3) and (4) each other on both sides with simple manipulation yields

$$\mathrm{T}_{round1} * \mathrm{T}_{round2} - T_{reply1} * T_{reply2} = \hat{T}_{\mathrm{prop}} * (4 * \hat{T}_{\mathrm{prop}} + 2 * T_{reply1} + 2 * T_{reply2}) \quad (5)$$

Adding Eqs. (3) and (4) on both sides with simple manipulation yields

$$\mathrm{T}_{round1} + \mathrm{T}_{round2} + T_{reply1} + T_{reply2} = 4 * \hat{T}_{\mathrm{prop}} + 2 * T_{reply1} + 2 * T_{reply2} \quad (6)$$

Combining (5) and (6), we can obtain $\hat{T}_{\mathrm{prop}}$ below,

$$\hat{T}_{\mathrm{prop}} = \frac{\mathrm{T}_{round1} * \mathrm{T}_{round2} - T_{reply1} * T_{reply2}}{\mathrm{T}_{round1} + \mathrm{T}_{round2} + T_{reply1} + T_{reply2}} \quad (7)$$

The dominant error in the ranging accuracy of this scheme is given by

$$\mathrm{error} = \frac{1}{4}(\mathrm{e}_B - \mathrm{e}_A) * \Delta T_{\mathrm{reply}} \quad (8)$$

Now we can see that dependence on T_{reply2} has been eliminated. The error is now dependent upon $\Delta T_{\mathrm{reply}}$, which is the difference between T_{reply1} and T_{reply2}. As long as T_{reply1} and T_{reply2} are kept as equal as possible, the propagation time error can be greatly reduced, which mainly comes from the frequency deviation of the crystal oscillator. Assuming the measured distance is 100 m, $\hat{T}_{\mathrm{prop}}$ will be 333 ns. If we use the crystal oscillator of 20 ppm, the error will be $20 * 10^{-6} * 333 * 10^{-9} = 6.7 * 10^{-12}$ s and the corresponding distance error is 2.2 mm [8].

3 Data Smoothing Method

In order to ensure sensitivity and obtain smoother data, a filtering algorithm is proposed combining a median filter and a Kalman filter. Before the data are sent to the Kalman filter for processing, the median filter is used to eliminate the jitter in order to obtain stable data quickly.

Firstly, we set 3 storage spaces (s_1, s_2, s_3) in memory and save three data d_{i-1}, d_i, d_{i+1} in these spaces, and then select the median among d_{i-1}, d_i and $, d_{i+1}$. But the refresh rate of this scheme is reduced by three times, from 20 samples per second to only 6–7 samples per second. To solve this problem, we put the median value of each output back into the storage space as data for the next comparison. Thus, the refresh rate is reduced by 10 samples per second.

Secondly, we designed a Kalman filter. Assume that the variables in the optimal estimation matrix $\hat{\mathrm{x}}_{\mathrm{k}}$ are random and obey the Gaussian distribution with mean μ and

variance σ^2. We predict the next state (k moment) from the current state (k-1 moment), and the prediction process is shown as

$$\hat{x}_k = F_k * \hat{x}_{k-1} \tag{9}$$

where F_k is a prediction matrix representing the state of the next moment, in which the variables are usually correlated. It can be expressed by covariance matrix P_k shown in Eq. (10) below. Each element in the matrix represents the correlation between the *i*th and the *j*th state variables.

$$P_k = F_k * P_{k-1} * F_k^T \tag{10}$$

If external interference is taken into account, the noise with covariance of Q_k should be added and Eq. (10) can be expressed as

$$P_k = F_k * P_{k-1} * F_k^T + Q_k \tag{11}$$

Because the sensor has noise, its uncertainty is expressed by covariance R_k and its mean value $\vec{z}_k$ is the sensor data we read.

Thus we have two Gaussian distributions, one near the predicted value (μ_0, σ_0^2) and the other near the sensor reading value (μ_1, σ_1^2). In order to find the optimal estimation in these two distributions, it is necessary to multiply the two Gaussian distributions to obtain the output of Kalman filter (μ', σ'^2).

$$k = \frac{\sigma_0^2}{\sigma_0^2 + \sigma_1^2} \tag{12}$$

$$\mu' = \mu_0 + k*(\mu_1 - \mu_0) \tag{13}$$

$$\sigma'^2 = \sigma_0^2 - k*\sigma_0^2 \tag{14}$$

According to Eqs. (12), (13), and (14) we can obtain $(\hat{x}_k, P_k)$ and $(\vec{z}_k, R_k)$.

$$K = P_k * (P_k + R_k)^{-1} \tag{15}$$

$$\hat{x}_k' = \hat{x}_k + K * (\vec{z}_k - \hat{x}_k) \tag{16}$$

$$P_k' = P_k - K*P_k \tag{17}$$

All in all, $\hat{x}_{k-1}$ and P_{k-1} are the optimal estimate of the previous moment. The estimate values $\hat{x}_k$ and P_k are obtained by the prediction process matrix F_k, and then updated to the optimal estimate value $\hat{x}_k'$ and P_k' by the measured readings. The optimal estimate can be iterated in the next prediction and updating equation.

4 Experiments and Analysis

We design UWB nodes based on DW1000 UWB chip [7] of DecaWave company in Ireland, using 2 nodes as base stations which are fixed on the support frame and 30 cm apart. With a node as label (target object) in hand, the experimenter moves away from the base station for 0.5 m to 6 m. At this time, the original data will generate 20–30 cm fluctuation. After the filter processing, relatively smooth data can be obtained. The experiment results are shown in Fig. 3.

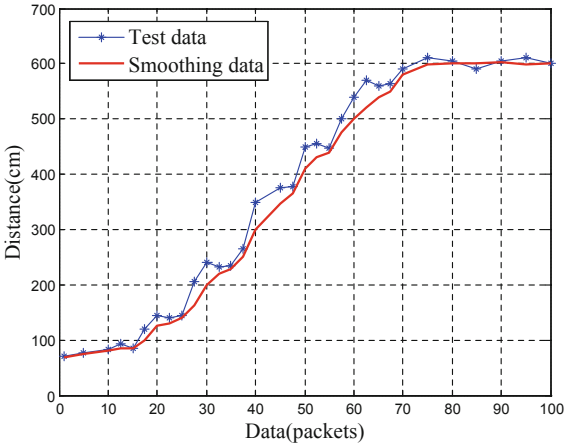

Fig. 3. Experiment data for 0.5 m to 6 m

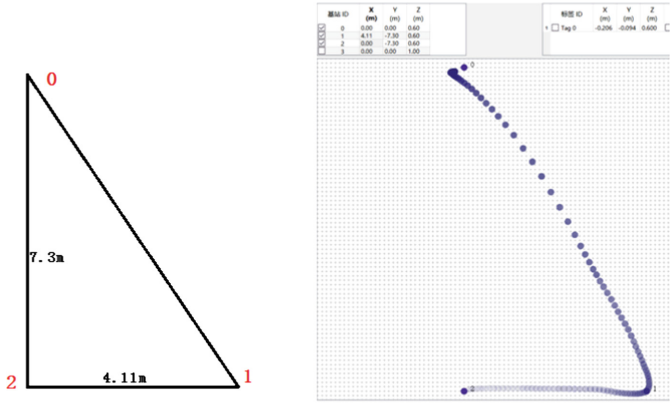

Fig. 4. Position of base stations and trajectories of the label

The indoor location test environment is shown in Fig. 4, including three base stations and one label. The coordinates of base stations 0, 1, and 2 are (0 m, 0 m), (4.11 m, −7.3 m) and (0.00 m, −7.3 m), respectively. Three base stations constitute a right triangle.

The hand tag moves straight from base station 2 to base station 1, and then goes straight to base station 0. The location trajectory is shown in Fig. 4. The indoor positioning experiment shows that the accuracy of the indoor positioning system can reach 10 cm except for the sloshing caused by walking.

5 Conclusion

In this paper, we design a high precision positioning method based on UWB technology. First, the symmetric double-sided two-way ranging method is used to reduce test error. Then, the algorithm combining a median filter and a Kalman filter is proposed to smooth data. The indoor real-time positioning system is realized by using weighted least square positioning algorithm at last.

In our future work, we will optimize the Kalman filter to process the system noise and measurement noise adaptively so as to improve the prediction accuracy. The scheme in this paper needs 2-way handshakes for positioning, and the number of target tags is limited. Next, TDOA will be adopted to further increase the number of object labels and reduce the power consumption of nodes.

References

1. Koyuncu, H., Yang, S.H.: A survey of indoor positioning and object locating systems. IJCSNS Int. J. Comput. Sci. Network Secur. **10**(5), 121–128 (2010)
2. Najera, P., Lopez, J., Roman, R.: Real-time location and inpatient care systems based on passive RFID. J. Network Comput. Appl. **34**(3), 980–989 (2011)
3. Zhang, D., et al.: Real-time locating systems using active RFID for Internet of Things. IEEE Syst. J. **10**(3), 1226–1235 (2014)
4. Fontana, R.J.: Recent system applications of short-pulse ultra-wideband (UWB) technology. IEEE Trans. Microwave Theory Tech. **52**(9), 2087–2104 (2004)
5. Salman, N., Rasool, I., Kemp, A.H.: Overview of the IEEE 802.15.4 standards family for low rate wireless personal area networks. In: 2010 7th International Symposium on Wireless Communication Systems, IEEE (2010)
6. Dardari, D., Closas, P., Djurić, P.M.: Indoor tracking: theory, methods, and technologies. IEEE Trans. Veh. Technol. **64**(4), 1263–1278 (2015)
7. DecaWave Ltd.: The implementation of two-way ranging with the DW1000. https://www.decawave.com/application-notes/. Accessed 23 Aug 2018
8. DecaWave Ltd.: Sources of Error in Two Way Ranging, https://www.decawave.com/application-notes/. Accessed 23 Aug 2018